

# A Comparative Study of the Effects of Rinsing and Aging of Polypyrrole/Nanocellulose Composites on Their Electrochemical Properties

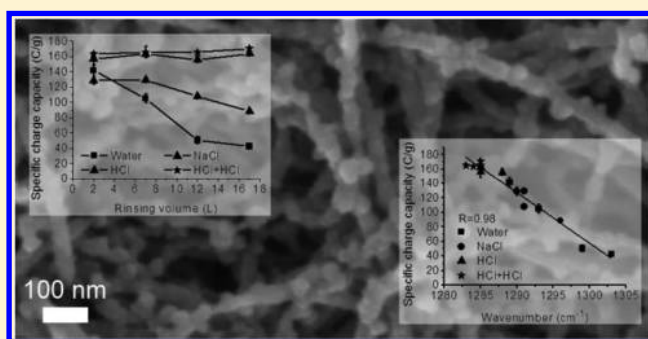
Daniel O. Carlsson,<sup>†</sup> Martin Sjödin,<sup>†</sup> Leif Nyholm,<sup>\*,‡</sup> and Maria Strømme<sup>\*,†</sup>

<sup>†</sup>Department of Engineering Sciences, Division of Nanotechnology and Functional Materials, The Ångström Laboratory, Uppsala University, Box 534, 751 21 Uppsala, Sweden

<sup>‡</sup>Department of Chemistry Ångström, The Ångström Laboratory, Uppsala University, Box 538, 751 21 Uppsala, Sweden

## S Supporting Information

**ABSTRACT:** The effects of polymerization conditions, rinsing, and storage on composites composed of polypyrrole (PPy) and Cladophora nanocellulose in terms of purity, chemical composition, conductivity, and electroactivity were investigated using conductivity measurements, cyclic voltammetry, FTIR-ATR, XPS, and ICP-AES. A clear correlation between rinsing volume and PPy degradation was found using water- or NaCl-rinsing solutions as evidenced by conductivity and electroactivity losses. It was further found, through FTIR-ATR as well as XPS-measurements, that this degradation was caused by incorporation of hydroxyl groups in the PPy-layer. The extent of degradation correlated with a shift in the FTIR-ATR peak around 1300 cm<sup>-1</sup>, showing that FTIR-ATR may be used as a quick diagnostic tool to evaluate the extent of degradation. By the use of acidic rinsing solution, this degradation effect was eliminated and resulted in superior samples in terms of both conductivity and electroactivity and also in a more efficient removal of reactants. Upon ambient storage, over a period of 200 days, a gradual decrease in conductivity was found for initially highly conductive samples. The electroactivity, on the other hand, was relatively unaffected by storage, showing that conductivity measurements alone are ineffective to determine the degree of polymer degradation if the water content is not controlled. Also, FTIR-ATR measurements indicated that the oxidation state did not change to any large extent upon storage and that only minor degradation of PPy occurred. The results presented herein thus offer valuable guidelines on how to develop simple and reliable postsynthesis treatments of conducting polymer–paper composites with performance fulfilling requirements on stability, electroactivity, and purity in applications such as environmentally friendly energy storage devices and biomedical applications.



## 1. INTRODUCTION

Electronically conducting polymers have been explored as functional materials in various applications, including batteries, light emitting diodes, photovoltaic cells, actuators, sensors, separation membranes, and controlled-release devices.<sup>1–3</sup> One of the most frequently studied conducting polymers is polypyrrole (PPy), which can be prepared through oxidative electrochemical or chemical polymerization of pyrrole, resulting in positively charged conducting polymer chains that are charge-compensated by counterions. The polymer is rendered nonconducting through reduction, which typically is coupled with expulsion of anionic counterions. The properties of the polymer, such as morphology, conductivity, and electroactivity, are influenced by the choice of counterion and solvent as well as electropolymerization method or oxidizing agent.<sup>1–8</sup> From an industrial point of view, chemical polymerization is preferred, as the process, unlike electrochemical polymerization, requires no conducting substrate and is more easily scaled up.<sup>2,3</sup> Particularly, chemical polymerization on cellulose

substrates is of interest because of the processability, low cost, and environmental friendliness of such substrates.<sup>2,3,9</sup>

We have recently described a composite material, where a thin layer of PPy (~30–50 nm) is coated, through chemical polymerization of pyrrole by FeCl<sub>3</sub>, onto highly crystalline (~95%) nanocellulose fibers with a large specific surface area (~90 m<sup>2</sup>/g) derived from Cladophora sp. algae.<sup>10</sup> It was found that the resulting electroactive and electrically conductive material retained the fibrous structure of the cellulose with a specific surface area comparable to the pure cellulose. The material has been investigated for use in energy-storage devices<sup>9,11–13</sup> as well as in biotechnological and biomedical applications, such as electrochemically controlled membranes for ion exchange,<sup>6,14,15</sup> including DNA-extraction<sup>16–18</sup> and hemodialysis.<sup>19,20</sup> Recently, we have also shown that PPy/

Received: December 20, 2012

Revised: March 11, 2013

Published: March 15, 2013

Table 1. Summary of Synthesis and Rinsing Conditions

batch name	sample name	0.4 M HCl added in synthesis	rinsing solution <sup>a</sup>	total rinsing volume (L)	rinsing time <sup>b</sup> (min)
Water	Water_2L	no	DI H <sub>2</sub> O	2	80
	Water_7L	no	DI H <sub>2</sub> O	7	210
	Water_12L	no	DI H <sub>2</sub> O	12	250
	Water_17L	no	DI H <sub>2</sub> O	17	280
NaCl	NaCl_2L	no	0.4 M NaCl (aq)	2	40
	NaCl_7L	no	0.4 M NaCl (aq)	7	110
	NaCl_12L	no	0.4 M NaCl (aq)	12	220
	NaCl_17L	no	0.4 M NaCl (aq)	17	280
HCl	HCl_2L	no	0.4 M HCl (aq)	2	50
	HCl_7L	no	0.4 M HCl (aq)	7	110
	HCl_12L	no	0.4 M HCl (aq)	12	185
	HCl_17L	no	0.4 M HCl (aq)	17	255
HCl+HCl	HCl+HCl_2L	yes	0.4 M HCl (aq)	2	35
	HCl+HCl_7L	yes	0.4 M HCl (aq)	7	105
	HCl+HCl_12L	yes	0.4 M HCl (aq)	12	170
	HCl+HCl_17L	yes	0.4 M HCl (aq)	17	230

<sup>a</sup>DI denotes deionized. <sup>b</sup>Total time the sample was immersed in the rinsing solution.

nanocellulose composites can be produced with porosities up to 98% and surface areas up to  $\sim 250 \text{ m}^2/\text{g}$ .<sup>21</sup>

For the realization of a PPy-based material in the above-mentioned applications, the material should be nontoxic as well as highly electroactive and stable while being manufactured in a cost efficient, easy, and environmentally friendly process.<sup>2</sup> Thus, working with aqueous solutions is preferred. In a recent report, it was shown that extensive rinsing with water and a subsequent extraction step in an aqueous buffer was necessary to render the PPy/cellulose composite noncytotoxic, but the rinsing led to significant electroactivity losses.<sup>20</sup> Less rinsing with water resulted in a material that was cytotoxic but exhibited higher electroactivity. These results show that the extent of rinsing of PPy-based materials is important for the safety and use of such materials, particularly in biomedical applications.

One problem associated with PPy-based energy-storage devices is self-discharge, and this has been suggested to be caused by, for example, mobile redox species present as impurities in the system.<sup>22,23</sup> The  $\text{Fe}^{3+}/\text{Fe}^{2+}$  redox couple present in the chemically synthesized polymer could potentially constitute one example of such species. Thus, residual iron from the PPy synthesis should be eliminated. Extremely long water rinsing procedures, up to a week, have been employed to remove iron from PPy powders,<sup>24–26</sup> but only a few groups have actually reported the iron content in their PPy powders (e.g., 0.34 wt %<sup>27</sup> and 0.3–0.4 wt %<sup>28</sup>). Further, water rinsing is one of the most common postsynthesis treatments of PPy powders, and is often described to be thorough, which implies that the rinsing is extensive but not necessarily well-controlled.

While extensive, and sometimes extreme, rinsing procedures with water have been employed, several reports on PPy degradation in aqueous solutions have also been put forward.<sup>25,26,29–43</sup> It has been suggested that the degradation consist of a fast overoxidation process and a slower process attributed to a nucleophilic attack by hydroxide ions on partially positively charged sites in the oxidized polymer.<sup>30,31</sup> It is conceived that the degradation stems from formation of hydroxyl and carbonyl groups in the PPy backbone, as shown through, for example, infrared spectroscopy (FTIR)<sup>33,34,37,39,40</sup> and X-ray photoelectron spectroscopy (XPS)<sup>32,35,38</sup> investigations. Even polymer chain breakage may occur as well as maleimide production.<sup>35,38,42</sup> The degradation leads to a

reduction of the PPy oxidation state, counterions are expelled, and the PPy conductivity and electroactivity is irreversibly reduced. The degradation is limited at low pH and high salt concentrations, while high pH and dissolved oxygen have been observed to accelerate the degradation.<sup>25,29,36,43</sup>

PPy conductivities have also been reported to decrease during ambient air aging and increased temperatures, which suggests degradation.<sup>25,44–47</sup> Oxygen and water present in the atmosphere, leading to similar modifications of the PPy backbone as the general mechanism of PPy degradation described above, has been suggested to be responsible for the conductivity losses.<sup>43–46</sup> Aging in more inert atmospheres has resulted in improved PPy stability.<sup>43,47</sup> Aging in ambient air, argon, and at  $-20^\circ\text{C}$  (air atmosphere) was also reported to lower the biocompatibility of PPy/cellulose composites, although argon and  $-20^\circ\text{C}$  aging offered some improvement as compared to ambient air.<sup>20</sup>

Thorough rinsing with water is commonly employed following PPy synthesis. However, to what extent rinsing with water affects conductivity, electroactivity, and the amount of residual iron in the polymer has not been reported in any detail previously. The aim of the current work was to carry out a comparative, extensive, and careful evaluation of how different rinsing solutions and extent of rinsing affect the conductivity, electrochemical, and structural properties of chemically synthesized PPy, deposited on cellulose substrates. Further, the PPy long-term stability in ambient air has also been investigated. In the past, PPy degradation during aging has primarily been evaluated through conductivity losses, while less attention has been paid to the electroactivity. Herein, these two indicators of degradation are compared. The long-term goal is to have a simple and reliable postsynthesis treatment of conducting polymer–paper composites with performance fulfilling requirements on stability, electroactivity, and purity in applications such as environmentally friendly energy storage devices and biomedical applications.

## 2. EXPERIMENTAL SECTION

**2.1. Materials.** Pyrrole (Merck),  $\text{FeCl}_3 \cdot 6\text{H}_2\text{O}$  (BDH Prolabo), Tween-80 (Merck), 37% HCl (Merck), and NaCl (BDH Prolabo) were used as received and diluted with deionized water to desired concentrations. *Cladophora* sp. algae

was collected, and the cellulose was prepared as described previously.<sup>48</sup>

**2.2. Sample Preparation.** Four batches of PPY/Cladophora cellulose composite samples were synthesized. For each batch, 400 mg of cellulose was dispersed in 70 mL of deionized water through high-energy ultrasonication (VibraCell 750W, Sonics, U.S.). Dissolved pyrrole and Tween-80 were added to the cellulose dispersion. FeCl<sub>3</sub> was then added, and the pyrrole was polymerized onto the cellulose fibers. Syntheses were carried out in 380 mL aqueous solutions with 0.17 M pyrrole, 0.12 M FeCl<sub>3</sub>, 0.06% Tween-80, 0.11% Cladophora cellulose, with stirring for 10 min. In one batch, the polymerization solution was made strongly acidic by the addition of HCl to a final concentration of 0.4 M, keeping the reaction volume constant. The products were transferred to a Büchner funnel and rinsed under reduced pressure with 2 L of the rinsing solution. To produce a series of samples identical in initial composition, each batch was then divided into four samples (parts), and each sample was rinsed separately with different amounts of the corresponding rinsing solution. One sample in each batch was not rinsed further. The second sample was rinsed with an additional 5 L, the third part with an additional 10 L, and the fourth part with an additional 15 L. Four batches, each containing four samples rinsed with different volumes and with three different rinsing solutions, were prepared. The rinsing solutions were deionized water, 0.4 M NaCl (aq), and 0.4 M HCl (aq). A summary of the synthesis and rinsing conditions for each sample under study is given in Table 1.

For FTIR-ATR reference samples, PPY powder was synthesized in the same way as described above for the sample named Water\_2L, cf., Table 1, without the addition of cellulose. A pure cellulose paper was produced by dispersing Cladophora cellulose as described above, and then collected and dried. All samples were stored in the ambient until analysis.

### 2.3. Characterization. 2.3.1. Conductivity Measurements.

*I*–*V* sweep measurements were performed at room temperature with a semiconductor device analyzer (B1500A, Agilent Technologies U.S.), and samples were cut into a rectangular shape with scissors. The length (*L*), width (*W*), and thickness (*T*) of the samples were in the ranges 0.90–1.05, 0.55–0.60, and 0.061–0.093 cm, respectively. Conductive silver paint was applied to the ends of the samples to ensure good contact between the samples and the needle probes. The potential (*U*) was scanned between –0.5 and 0.5 V, and the current (*I*) was recorded. The conductivity ( $\sigma$ ) was calculated from the conductance  $\Delta I/\Delta U$  by  $\sigma = (\Delta I/\Delta U)(L/WT)$ . For each sample, nine measurements were made at three different times after synthesis.

**2.3.2. CV Measurements.** Cyclic voltammograms were recorded versus an Ag/AgCl 3 M NaCl (aq) reference electrode with a platinum wire counter electrode in a three-electrode setup. The samples were mounted on a platinum wire shaped like a paper clip and employed as the working electrode. All measurements were performed in 2.0 M NaCl (aq) with 5 mV/s scan rate controlled by an Autolab potentiostat (Eco Chemie, The Netherlands). For each sample, two or three measurements were made at three different times after synthesis. The potential was scanned between –0.6 and  $\geq +0.3$  V. The charge capacity was calculated from the anodic scans by integrating the current from the first point of positive current to 0.3 V and normalized by sample weight (samples weighed 1.3–3.3 mg).

Composite reference samples for FTIR-ATR were prepared by three-electrode CV cycling of a Water\_2L sample using the same setup as described above. Two sets of reference samples were produced. In one set, samples were cycled for 4 and 8 times up to +0.3 V vs Ag/AgCl in a solution with 2 M NaCl and 0.01 M NaOH (pH  $\sim 12$ ). In another set, an increasing number of cycles (1–50) up to 1.05 V vs Ag/AgCl was performed in 2 M NaCl to electrochemically overoxidize the samples.

**2.3.3. FTIR-ATR Spectroscopy.** FTIR-ATR spectra were recorded on a Spectrum One FTIR spectrometer equipped with a Diamond/ZnSe crystal (PerkinElmer, U.S.). The resolution was set to 4 cm<sup>–1</sup>, and 40 scans were averaged. Duplicates of each sample were analyzed at three different points in time, and peak positions were determined by the Spectrum software (PerkinElmer, U.S.). For comparison purposes, intensities have been shifted in the figures, keeping the relative intensities constant.

**2.3.4. XPS.** High-resolution XPS spectra for C, N, O, and Cl were obtained with a Phi Quantum 2000 (Physical Electronics, U.S.) equipped with an Al K $\alpha$  source (1486.6 eV, 45 W). The analyzer was operated at 23.5 eV pass energy, and electron and Ar<sup>+</sup> gun neutralization was applied to minimize charging effects. Spectra were reduced with a Shirley background, and elemental atomic concentrations and ratios were calculated from the XPS peak areas, employing sensitivity factors included in the Multipak software (Physical Electronics, U.S.). Binding energies were shifted and referenced to the C1s peak at 285.00 eV to allow easy comparison with reference data.<sup>49</sup> In the figures, the intensities have been normalized with respect to the corresponding maximum intensity for easier comparison of samples.

## 3. RESULTS

**3.1. Effects of Rinsing.** PPY/cellulose composites were synthesized and rinsed with water, 0.4 M NaCl (aq), or 0.4 M HCl (aq) (see Table 1), and the effects of the different rinsing solutions were characterized with conductivity measurements, electroactivity determinations, FTIR-ATR, XPS, and ICP-AES.

**3.1.1. Conductivity.** The effect of rinsing with varying amounts of the different solutions on the conductivity of fresh composite samples is shown in Figure 1. A distinct conductivity decrease was observed with increased volumes of both water

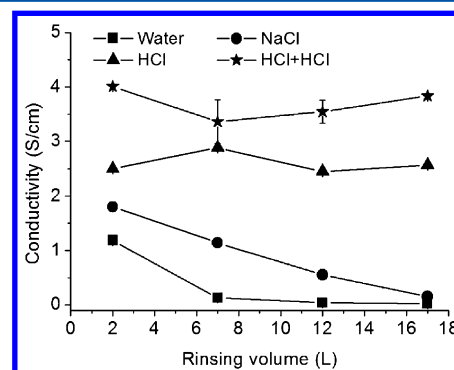


**Figure 1.** Conductivity of PPY/cellulose composite samples as a function of rinsing volume. The values presented are average values of nine measurements, and the error bars represent the standard deviation. For most data points, the error bar is smaller than the size of the symbol.



and NaCl (aq), while stable conductivities in both batches of samples rinsed with HCl (aq) were observed. After rinsing with 17 L of water, 2% of the conductivity that was measured after 2 L of water rinsing remained. The corresponding values for the NaCl, HCl, and HCl+HCl batches were 9%, 102%, and 96%, respectively.

**3.1.2. Electroactivity.** Cyclic voltammetry was performed in 2 M NaCl (aq) in a three-electrode setup (voltammograms are shown in Figure S1 in the Supporting Information). Specific charge capacities for all samples, shown in Figure 2, were

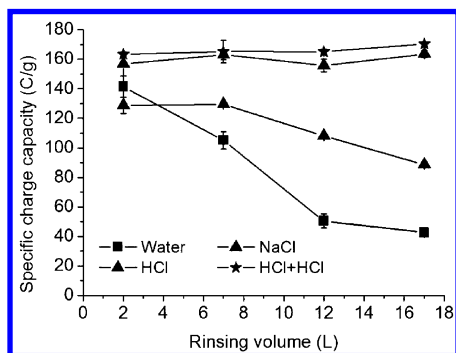


**Figure 2.** Specific charge capacities of all PPY/cellulose composite samples, calculated from the first anodic scan, as a function of rinsing volume. The values presented are average values of two measurements, and the error bars represent the absolute deviation. For some data points, the error bar is smaller than the size of the symbol.

calculated from the first cycle voltammograms and taken as a measure of electroactivity. For the water-rinsed samples, decreased charge capacities with increasing rinsing volumes were observed. A similar behavior, although not as prominent, was observed also in the NaCl batch. The decrease in electroactivity was accompanied by a shift in oxidation peak potential toward more positive potentials. The HCl and HCl+HCl batches displayed stable, volume-independent, charge capacities as well as constant peak potentials. When comparing the charge capacity of the samples rinsed with 17 L with samples rinsed with 2 L of the corresponding solution, the capacity qualitatively followed the same trend as the fading of the conductivity for the Water (30% charge capacity retention) and NaCl (69%) batches. For the HCl and HCl+HCl batches, the charge capacity retention was 104% and 104%, respectively.

To investigate the reversibility of the reduced electroactivity of the Water and NaCl, the samples were cycled 50 or 100 times in 2 M NaCl, and the charge capacity of each cycle was calculated as above. Selected samples rinsed with HCl (aq) were analyzed accordingly. The relative charge capacities for each sample (defined as the charge capacity of a certain cycle divided by the charge capacity of the first cycle) versus cycle number are shown in Figure 3. All samples rinsed with HCl and the Water\_2L and NaCl\_2L samples displayed a steady decrease throughout the experiment. Samples rinsed with  $\geq 7$  L of water or 0.4 M NaCl (aq), on the other hand, displayed an initial increase in their relative charge capacities, followed by a steady decrease in similarity with the HCl-rinsed samples. The number of cycles under which the increase occurred increased as the rinsing volume was increased. In general, the number of cycles under which the increase was observed was larger after water rinsing than for the corresponding NaCl (aq)-rinsed samples.

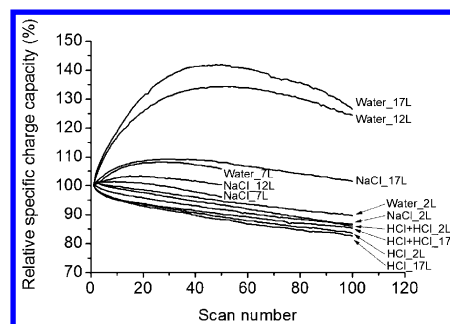


**Figure 3.** Relative specific charge capacities (with respect to the charge capacity of the first cycle) of PPY/cellulose composites during CV-cycling as a function of the cycle number.

**3.1.3. FTIR-ATR.** Figure S2 in the Supporting Information shows the FTIR-ATR spectra in the range 1900–650  $\text{cm}^{-1}$  of all samples in the Water batch and of the samples rinsed with 2 and 17 L in the other three batches. Spectra of a Cladophora cellulose membrane and PPY powder are also shown in the same figure. All composite spectra resemble that of pure PPY powder and contain the typical PPY peaks<sup>50</sup> with no contributions from the cellulose framework. It can further be observed that no spectral changes as a result of acidic rinsing occurred, whereas several gradual spectral changes occurred as a result of increased volumes of water or 0.4 M NaCl (aq) rinsing, with the latter displaying changes to a lesser degree than the former. Two of the gradual changes were peak position shifts toward higher wavenumbers and/or widening of a majority of the peaks (Table S1 in the Supporting Information), and evolution of a shoulder on the high wavenumber side (at  $\sim 1060 \text{ cm}^{-1}$ ) of the peak at  $1030 \text{ cm}^{-1}$  (highlighted in Figure 4). An example of the peak shifts is the

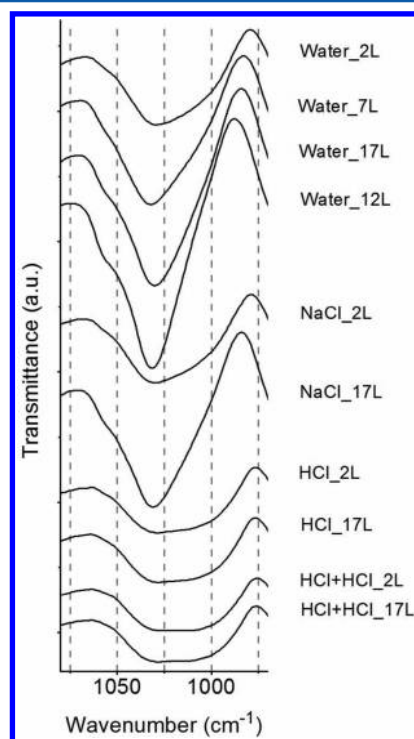


**Figure 4.** FTIR-ATR spectra of all samples in the Water batch and the samples rinsed with 2 and 17 L in the NaCl, HCl, and HCl+HCl batches in the region 1080–970  $\text{cm}^{-1}$ .

shift of the peak around  $1300\text{ cm}^{-1}$ , which correlated with the specific charge capacity of the samples, as can be seen in Figure 5 (charge capacities from Figure 2).

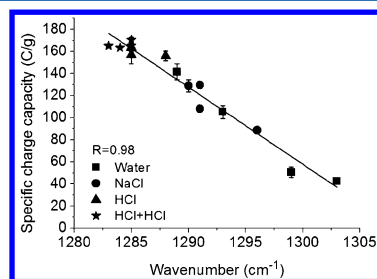


**Figure 5.** Specific charge capacity of the PPY/cellulose composites as a function of the peak position of the FTIR-ATR peak around  $1300\text{ cm}^{-1}$ . Error bars represent the absolute deviation of two measurements and are in some cases smaller than the symbol.

Two composite reference sets were produced by performing cyclic voltammetry with samples rinsed with 2 L of water and analyzed in FTIR-ATR accordingly. In the first set, the pH of the 2 M NaCl (aq) electrolyte solution was adjusted to  $\sim 12$  with NaOH, and samples were cycled for 4 and 8 cycles up to 0.3 V, that is, nonoveroxidizing potentials. For each scan, the oxidation potential shifted toward more positive potentials and the currents decreased. The FTIR-ATR spectra (see Figures S3 and S4 in the Supporting Information) displayed the same gradual changes as after rinsing with water or 0.4 M NaCl (aq), that is, peak shifts and the development of a shoulder in the peak at  $1030\text{ cm}^{-1}$ .

In the second reference set, composite samples were cycled 1–50 cycles up to +1.05 V in a neutral 2 M NaCl solution to produce overoxidized samples. For each cycle, the oxidation peak shifted in the positive direction and currents decreased. The resulting gradual FTIR-ATR spectra changes (see Figures S3 and S4 in the Supporting Information) included peak shifts, particularly seen after 1 and 5 scans, but the spectra did not display a similar shoulder in the  $1030\text{ cm}^{-1}$  peak as observed with water or 0.4 M NaCl (aq)-rinsed samples or the samples in the other reference set. Instead, the peak gradually changed in appearance, first by shifting in position toward higher wavenumbers and eventually splitting into multiple peaks. After the first scans, a peak at  $\sim 1700\text{ cm}^{-1}$  evolves and continues to grow in intensity up until 15–20 overoxidation scans.

**3.1.4. XPS.** The XPS C1s spectra are shown in Figure 6 for samples rinsed with 2 and 17 L in each batch. No significant difference was observed between any samples rinsed with 2 or 17 L of the same solution. However, as compared to the samples rinsed with HCl, the samples rinsed with water or NaCl displayed a distinct shoulder around 286.5 eV.

In Figure 7, the relative oxygen (O1s) and chloride (Cl2p) atomic concentrations (with respect to the nitrogen, N1s, content) are shown. No significant difference in oxygen and chloride content between the HCl-rinsed samples could be observed. The oxygen content of the samples in the Water and NaCl batches was significantly higher. For these samples, the oxygen content of the samples rinsed with 17 L was also higher than the corresponding samples rinsed with 2 L. In terms of chloride content in the Water and NaCl samples, the samples rinsed with 2 L contained more chloride than the corresponding sample rinsed with 17 L.

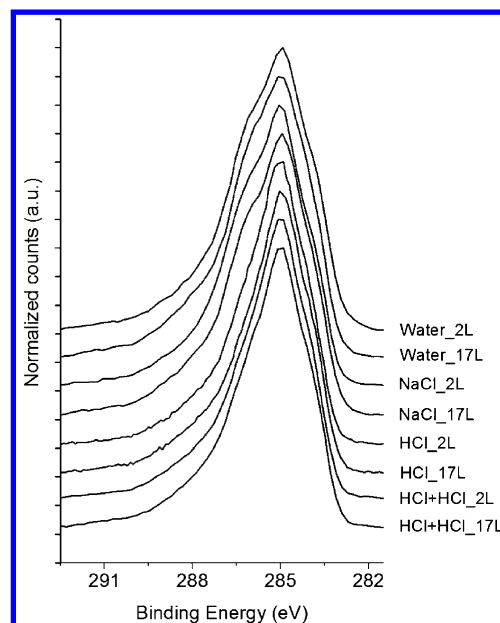


**Figure 6.** XPS C1s spectra of PPY/cellulose composite samples rinsed with 2 or 17 L of the corresponding rinsing solution.

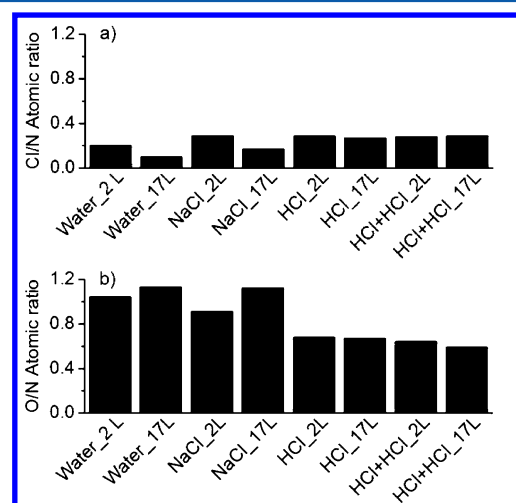


**Figure 7.** XPS Cl to N (a) and O to N (b) atomic ratios of PPY/cellulose composites.

**3.1.5. Total Iron Content.** The total iron content, determined through ICP-AES, is summarized in Table 2 for

**Table 2. Total Iron Content per Gram Sample after Rinsing with 2 and 17 L of the Corresponding Rinsing Solution**

	[Fe] after 2 L rinsing ( $\mu\text{g/g}$ )	[Fe] after 17 L rinsing ( $\mu\text{g/g}$ )
Water	1770	1500
NaCl	2050	1920
HCl	863	211
HCl+HCl	479	159

the samples rinsed with 2 and 17 L in each batch. In the Water and NaCl batches, only a minor decrease in iron content was observed as the rinsing volume was increased. Seventeen liters of acidic rinsing resulted in 1 order of magnitude lower iron content than the corresponding samples from the Water and NaCl batches. The iron content of the analyzed samples ranged

from  $\sim 160$ – $2050 \mu\text{g Fe}$  per gram sample, that is,  $0.016$ – $0.21 \text{ wt } \%$ . Assuming that all iron was located within the PPy layer of the composites and the fact that composites prepared according to the same protocol consisted of  $54 \text{ wt } \%$  PPy,<sup>51</sup> these values correspond to an iron content of  $0.029$ – $0.38 \text{ wt } \%$  within the PPy layer.

**3.2. Effects of Aging in Ambient Air.** The effects of aging were investigated employing conductivity measurements, electroactivity measurements, and FTIR-ATR.

**3.2.1. Conductivity.** The effect of long-term storage in the ambient on the conductivity is summarized in Figure 8, for

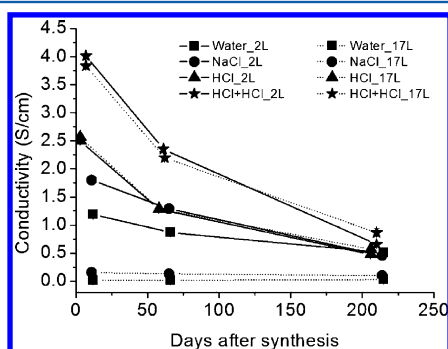


**Figure 8.** Conductivity of PPy/cellulose composite samples as a function of storage time in the ambient for samples rinsed with 2 or 17 L in each batch. The values presented are average values of nine measurements, and the error bars represent the standard deviation. The error bar is smaller than the symbol for most samples.

samples rinsed with 2 or 17 L in each batch. Irrespective of the rinsing solution and volume, there was generally a significant loss of conductivity upon storage, except for samples Water\_17L and NaCl\_17L, which already, as a result of the extensive rinsing, had very low conductivities. It can also be seen that, except for samples Water\_17L and NaCl\_17L, the conductivities decreased toward a common value with aging time. Specifically, the HCl-rinsed samples lost 77–84% of their initial conductivity over the time period of approximately 200 days.

**3.2.2. Electroactivity.** The electroactivity was evaluated through the specific charge capacities, as described above. In Figure 9, it can be observed that no major decrease in charge

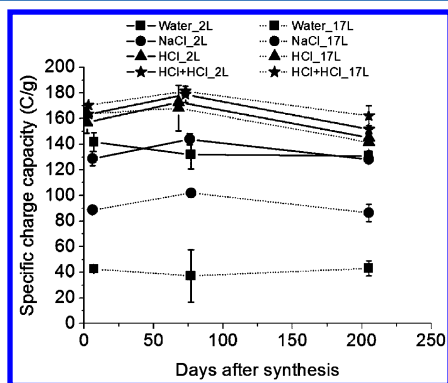


**Figure 9.** Specific charge capacities for samples rinsed with 2 or 17 L in each batch as a function of time. The error bars represent the absolute deviation of two (at  $t = 2$ – $7$  days and  $t = 70$ – $80$  days) and three (at  $t = 210$  days) measurements. The error bars are in some cases smaller than the symbol.

capacity occurred over the time period of approximately 200 days for any sample. For example, the HCl-rinsed samples lost 4–14% of their initial charge capacity. A weak, but notable, storage time dependence could, however, be observed for a majority of the samples under study, involving a small increase in charge capacity over the first 70–80 days, followed by a small decrease.

**3.2.3. FTIR-ATR.** FTIR-ATR spectra of selected samples (Water\_2L, Water\_17L, HCl+HCl\_2L, and HCl+HCl\_17L) over approximately 200 days are shown in Figure S5 in the Supporting Information. For the samples that were not significantly degraded during rinsing (i.e., Water\_2L, HCl+HCl\_2L, and HCl+HCl\_17L), shifts corresponding to  $5$ – $7 \text{ cm}^{-1}$  were seen for the peak at  $1300 \text{ cm}^{-1}$ , while Water\_17L only displayed a small shift ( $2 \text{ cm}^{-1}$ ) over the time period (Table 3). During the aging, the peak at  $1030 \text{ cm}^{-1}$  changed in

**Table 3.** Position of the Peak (in  $\text{cm}^{-1}$ ) around  $1300 \text{ cm}^{-1}$  for Selected Samples at Different Times (Number of Days) after Synthesis

	12 days	77 days	207 days
Water_2L	1289	1294	1296
Water_17L	1303	1302	1305
	7 days	72 days	206 days
HCl+HCl_2L	1284	1288	1290
HCl+HCl_17L	1285	1287	1290

appearance to some extent in the samples, as shown in Figure 10. In both of the Water samples, but particularly in Water\_17L, a peak at  $1700 \text{ cm}^{-1}$  evolved with time, and the intensity increased throughout the investigated time period.

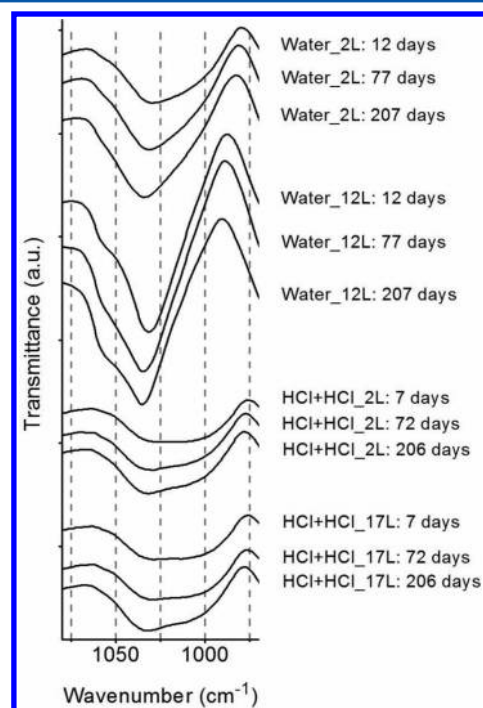


**Figure 10.** FTIR-ATR spectra in the region  $1080$ – $970 \text{ cm}^{-1}$  of samples Water\_2L, Water\_17L, HCl+HCl\_2L, and HCl+HCl\_17L recorded 7–12, 72–77, and 206–207 days after synthesis and aging in the ambient.



This peak was not observed in the HCl+HCl samples after ~200 days of ambient storage.

## 4. DISCUSSION

Before the results concerning PPy degradation during rinsing and aging are discussed, the iron removal efficiency will be discussed briefly (see Table 2). The iron removal with water, as well as with NaCl (aq), was ineffective, confirming earlier reports where extensive washing with water was needed to remove iron.<sup>24–26</sup> Acidic rinsing resulted in 10-fold lower quantities of iron, as compared to water rinsing. The iron content of the PPy-layer following 17 L of acidic rinsing was also approximately an order of magnitude lower than what has previously been reported for pure PPy powders.<sup>27,28</sup> The explanation for the more efficient iron removal is the pH-dependent solubility of iron species, where a near neutral pH of the rinsing solution results in iron-containing precipitates in the material.

Besides resulting in a lower iron content in the material, acidic rinsing did not reduce the conductivity and electroactivity, unlike the two neutral rinsing solutions (see Figures 1 and 2). This agrees well with the consensus that PPy degradation is pH-dependent. Upon degradation of the polymer, the positive charge of the polymer is consumed and the distribution of charges within the polymer is changed as well as the concentration of counterions. The hallmarks of PPy degradation are considered to be the hydroxyl and carbonyl groups that form in the polymer skeleton. The conjugation length of the polymer may be changed, and the conductivity and electroactivity are irreversibly reduced. In the following, the effects of acidic rinsing are discussed followed by a discussion concerning the degradation of the composite PPy-layer during nonacidic rinsing and ambient air storage.

**4.1. Effects of Acidic Rinsing.** The data presented in Figures 1 and 2 show that by using a rinsing solution of low pH, the PPy/cellulose composites can be extensively rinsed without reducing the conductivity or electroactivity. This also shows that the PPy-coating on the cellulose fibers is stable and withstands extensive rinsing, as PPy detachment would have resulted in lowered specific charge capacities. The FTIR-ATR data (Figures 4 and 5, and Figure S2 and Table S1 in the Supporting Information), which reflect PPy backbone modifications and oxidation state of the polymer, confirm the observed nondegrading effects of acidic rinsing as no spectral changes were observed as a result of rinsing volume. That the oxidation state of the composites is unaffected is also confirmed by the chloride content determinations from XPS data (Figure 7). The ratio between the chloride and nitrogen content is approximately 0.3, which reflects the total chloride content, and this would be expected to decrease in case of degradation.

It should also be mentioned that two batches, one in which the polymerization reaction was performed under extra acidic conditions (the HCl+HCl batch), were rinsed with 0.4 M HCl, and both were unaffected by the extent of rinsing. There was no significant difference in terms of electroactivity between the two batches (Figure 2), showing that the resulting amount of PPy was not significantly affected by the addition of HCl in the synthesis. However, there is a significant difference in conductivity between the two batches. This difference cannot be attributed to the rinsing step because it was identical in the two cases, but it can be concluded that highly acidic polymerization conditions results in a higher quality polymer material. In neither of these batches could PPy degradation be

observed, and it can be concluded that acidic rinsing provides a route toward highly electroactive, conducting, stable, and potentially noncytotoxic PPy/cellulose composites, as well as more efficient residual iron removal.

**4.2. Degradation of PPy/Cellulose Composites.** The samples rinsed with HCl were superior in all investigated properties as compared to the samples rinsed at neutral pH. Although not specifically studied, it should be considered that oxygen must have been dissolved in all rinsing solutions, and yet no degradation was observed as a result of acidic rinsing. This indicates that the accelerated degradation observed in previous reports<sup>30,44</sup> due to dissolved oxygen must be more complex than straightforward oxidation of PPy by a strong oxidizing agent, particularly because oxygen is a stronger oxidizing agent at low pH. It thus seems that also the degrading effects of dissolved oxygen are favored by higher pH. It can be speculated that this is due to either limited reaction kinetics at low pH or a lack of a required precursor. In the following sections, the important parameters affecting the degradation (pH and salt) will be discussed, with reference to HCl rinsing, as well as the reversibility of the degradation.

**4.2.1. Influence of pH on Degradation.** The data in Figure 1 and 2 show that the degradation during nonacidic rinsing is gradual; that is, the degradation is volume-dependent (or time-dependent). This is also supported by the observed decrease in the number of chloride ions when comparing the chloride content of the 2 and 17 L-rinsed samples (Figure 7). This indicates that the number of positive charges in PPy has decreased as a result of increased rinsing volumes. Carbonyl and hydroxyl groups, attached to the polymer backbone, are commonly associated with PPy degradation,<sup>32–35,37–40</sup> and it would be anticipated that the number of carbonyl and hydroxyl groups in the polymer backbone should increase gradually if the degradation is gradual. Indeed, in the FTIR-ATR spectra of the overoxidized reference samples (Figure S3, Supporting Information), prepared through overoxidative CV-cycling, a gradual increase of a peak at  $\sim 1700\text{ cm}^{-1}$  is observed as the number of overoxidation scans is increased, which can be attributed to carbonyl groups.<sup>39</sup> A careful examination of the spectra at  $1700\text{ cm}^{-1}$  (close to the detection level) does not indicate a significant difference between samples rinsed with 2 or 17 L of water or 0.4 M NaCl (aq). This suggests that the number of carbonyl groups present in all of these samples is low. The FTIR-ATR spectra should, however, be interpreted with care, because the intensity of the peaks will be a function of, for example, the complex refractive index,<sup>52</sup> which for PPy varies depending on oxidation state.<sup>53</sup> In this case, a reduced oxidation state generally results in higher peak intensities. The XPS C1s spectra (Figure 6), however, also indicate that the number of carbonyl groups (binding energy  $288\text{ eV}^{49}$ ) is low and that no significant difference between any of the samples, including the HCl-rinsed samples, can be observed. Thus, even though as much as 98% of the conductivity and 70% of the electroactivity has been lost as a result of rinsing with 17 L of water, neither FTIR-ATR nor XPS indicates a significant increase in the number of carbonyl groups. This suggests that carbonyl functionalities present in the polymer backbone are not a satisfactory explanation for the degradation.

The only significant difference in the XPS C1s spectra (Figure 6) between samples rinsed with acidic and nonacidic rinsing solutions was the shoulder around  $286.5\text{ eV}$ , attributed to C–O bonds.<sup>49</sup> This indicates that on the very surface (outer few nanometers), samples rinsed with nonacidic solutions have

a higher amount of hydroxylated PPy than samples rinsed with acidic solutions. In FTIR-ATR, which typically probes a few micrometers into the sample, the shape of the peak at  $1030\text{ cm}^{-1}$  was particularly influenced by electrochemical over-oxidation but also by CV-cycling at pH 12 (Figure S4 in the Supporting Information) as well as rinsing with nonacidic solutions (Figure 4). These changes were gradual, as one would expect due to gradual degradation by either electrochemical cycling or nonacidic rinsing. Alkaline treatment<sup>36</sup> and over-oxidation<sup>35</sup> are both known to introduce hydroxyl groups in the PPy backbone. As the peak at  $1030\text{ cm}^{-1}$  is highly influenced by such treatments, the observed changes in rinsed samples, that is, gradual evolution of a shoulder around  $1060\text{ cm}^{-1}$ , are most likely due to an increased presence of C–O, that is, C–OH, in the structure. It should also be noted that the gradual change of the  $1030\text{ cm}^{-1}$  peak, observed as a result of nonacidic rinsing, is identical to those observed during CV-cycling at pH 12, whereas the change imposed by overoxidation was different with a clear separation of the peak into multiple separate vibrations. These results suggest that the degradation of the composite samples due to rinsing with water or 0.4 M NaCl (aq) mainly is due to formation of hydroxylated PPy, rather than carbonyl groups.

It is known that the positions of IR-peaks of conducting polymers depend on the oxidation state and conjugation length of the polymer.<sup>50</sup> In FTIR-ATR, the peak position will also be affected by the complex refractive index of the polymer,<sup>52</sup> which varies depending on the oxidation state of the polymer.<sup>53</sup> As found in the present investigation, a majority of the PPy peaks shifted toward higher wavenumbers as a result of rinsing-induced degradation (Table S1 in the Supporting Information), showing that the number of positive charges within the PPy-layer decreased as a result of extended rinsing with water or 0.4 M NaCl. Specifically, the position of the peak around  $1300\text{ cm}^{-1}$ , reflecting the average oxidation state of the PPy-layer, was found to correlate with the extent of degradation, as measured by the remaining specific charge capacity (Figure 5). This correlation may be used as a quick way to evaluate the extent of PPy degradation following different treatments.

**4.2.2. Influence of Salt on Degradation.** So far, the discussion has been focused on the pH-dependent degradation of the PPy-layer in the composites, while the effect of salt has not been discussed. In Figure 2 it can be observed that in terms of electroactivity the presence of NaCl in the rinsing solution has a protective effect, as compared to pure water. Other groups have also observed similar effects by the addition of salts during immersion experiments<sup>25,29</sup> but have to our knowledge not confirmed these results with spectroscopic data. Here, the protective effect of NaCl could be confirmed by FTIR-ATR where the previously discussed peak shifts were not as profound as with water (Figure 5, and Table S1 in the Supporting Information), indicating a higher oxidation state, and hence less degradation. Further, the shoulder in the  $1030\text{ cm}^{-1}$  peak (Figure 4), attributed to the presence of hydroxyl groups, was likewise not as profound as with water. Thus, it can be concluded that salt indeed protects PPy from degradation, although 0.4 M NaCl (aq) did not completely inhibit degradation. It is possible that an even higher salt concentration could reduce the extent of degradation further, given that others have observed that the loss of conductivity was reduced as the salt concentration was increased.<sup>25</sup>

Although the mechanism of protection of the salt is unknown, it could be interesting for the elucidation of the

mechanism to note that the C1s spectra of the samples rinsed with 2 and 17 L are identical (Figure 6). This was also true for the water-rinsed samples. This means that there is no significant difference in the amount of oxygen covalently bound to carbon. At the same time, there are differences in the total oxygen content (Figure 7), with the most rinsed samples having the highest oxygen content, suggesting that there could be oxygen-containing species present in the film that are not covalently bound to carbon. It should, however, be remembered that XPS only probes the top few atomic layers of the material and that this does not necessarily reflect the bulk properties.

**4.2.3. Reversibility of Degradation.** It was observed for samples rinsed with 7 L or more with water or 0.4 M NaCl (aq) that the charge capacity increased under a number of cycles (Figure 3). This is due to shifts of the oxidation peak toward more negative values while the currents increase for each scan, which means that a larger area is integrated when calculating the charge capacity. It can further be observed in Figure 3 (1) that the duration of this effect was related to the extent of rinsing with neutral solutions and (2) that the duration was shortened by the addition of 0.4 M NaCl (aq). This shows that the degrading effects of rinsing with water or 0.4 M NaCl (aq) to some extent can be reversed and the samples reactivated. It should, however, be pointed out that in terms of absolute recovery of the electroactivity, these effects were very modest (corresponding to approximately 3–15 C/g), which means that the irreversible effects of rinsing with water or 0.4 M NaCl (aq) are dominating.

Following the varying periods of reactivation, the electroactivity of the samples started to decrease as the number of scans increased (Figure 3), as did the HCl-rinsed samples throughout the experiment. Loss of electroactivity during cycling has been observed previously and attributed to  $\text{OH}^-$  in the electrolyte and its attack on PPy.<sup>12</sup>

**4.3. Degradation during Long-Term Storage in Ambient Air.** Focusing first on the samples that already during rinsing became severely degraded, for example, Water\_17L, it can be seen that the very low conductivity is stable throughout the time period of approximately 200 days (Figure 8), and this is also true for the electroactivity (Figure 9). The FTIR-ATR peak at  $\sim 1300\text{ cm}^{-1}$  (see earlier discussion) remains relatively unaffected, and only a small shift toward higher wavenumbers can be seen (Table 3), showing that the oxidation state has not been changed to any larger extent. This shows that the degradation of already severely degraded samples is limited during storage in the ambient, which is reasonable given that such samples have fewer positive charges.

Although the oxidation state of Water\_17L does not change to any large extent during the aging and no significant degradation could be observed, there is a clear increase in the intensity of a carbonyl peak at  $1700\text{ cm}^{-1}$  in the IR spectra with time (Figure S5 in the Supporting Information). This shows that the number of carbonyl functionalities increases with storage time and that this has no significant effect on the conductivity and electroactivity properties of the composite. Also, in Water\_2L a carbonyl peak is seen to develop, although weaker as compared to Water\_17L, whereas this is not observed for the HCl+HCl samples, which indicates that the number of carbonyl groups in the latter case remains low, even after >200 days of ambient storage.

For the samples that have not been severely degraded during rinsing, for example, HCl+HCl samples, only minor changes in FTIR-ATR spectra could be observed (Figure S5 in the



Supporting Information). The  $1300\text{ cm}^{-1}$  peak shifts slightly toward higher wavenumbers (Table 3), indicating that the oxidation state of PPy is reduced to some extent, which in turn suggests that minor degradation has occurred during  $\sim 200$  days of storage in the ambient. The  $1030\text{ cm}^{-1}$  peak also changes in appearance (Figure 10), which could indicate formation of hydroxyl groups in the PPy-layer. However, no shoulder is seen as was the case after rinsing with nonacidic solutions. It was shown above that along with the evolution of the shoulder there was a general shift of peaks toward higher wavenumbers, and it may be that the peak corresponding to C–O, that is, C–OH, has not shifted sufficiently to produce a peak with a high wavenumber shoulder.

In terms of electroactivity, a loss corresponding to 4–14% over the same time period,  $\sim 200$  days, could be observed (Figure 9) and confirms that the degradation occurring during storage is limited. A weak, but notable, storage time dependence can, however, be revealed for a majority of the samples under study with a small increase in charge capacity over the first 70–80 days followed by a small decrease. The charge capacities are normalized by weight (samples were weighed prior to measurement), and a possible explanation for the observed initial increase is reduced water content in the samples, resulting in an increased gravimetric capacity, which compensates a slow degradation process.

The conductivity data (Figure 8) show that all samples approach a common value, that there is a leveling off effect, which shows that the choice of rinsing solution has little impact on the conductivity after a long storage time in the ambient. Specifically, the data suggest that the degradation is extensive, with losses corresponding to 77–84% for the HCl+HCl samples. This may seem surprising given that both the electroactivity and the FTIR-ATR data show that the degradation is not very extensive. In addition, the FTIR-ATR data indicate that the oxidation state has not been changed to any large extent, which also means that any self-discharge process occurring during storage should be limited. However, the conductivity is governed by the oxidation state of PPy, which is reduced due to degradation, but also by the aqueous phase within the material.<sup>3,10</sup> In particular, it is known that the conductivity of PPy/cellulose composites will increase significantly with increased water content.<sup>10</sup> Therefore, the results demonstrate that unless the water content of the samples is controlled, conductivity will be a poor measure of PPy degradation.

## 5. CONCLUSIONS

The objective of this investigation was to carry out a careful investigation of how different postsynthesis treatments affected both the short-term and the long-term properties of the PPy/nanocellulose composite. The synthesis process, based on oxidation by  $\text{Fe}^{3+}$ , produced a complete PPy coverage of the nanocellulose fibers. Synthesis with the addition of HCl did not affect the electroactivity but resulted in higher conductivities. Rinsing with HCl as a postsynthesis treatment reduced the iron contamination of the PPy/cellulose composite considerably as compared to when nonacidic rinsing was employed and was an order of magnitude lower than previously reported values for pure PPy powders.

The HCl-rinsed samples were superior to the nonacidic-rinsed samples in terms of conductivity and electroactivity. The conductivity and electroactivity did not change with extensive

acidic rinsing, and no PPy detachment or degradation occurred during rinsing as confirmed with FTIR-ATR and XPS.

It was confirmed that PPy degradation is pH dependent. It was further shown that the extent of degradation was dependent on the volume of rinsing with nonacidic solutions. No compelling evidence was, however, found for significant amounts of carbonyl groups in the PPy-layer, even though 98% of the conductivity and 70% of the electroactivity had been lost after 17 L of water rinsing. Instead, FTIR-ATR and XPS data indicated that the degradation is caused by incorporation of hydroxyl groups in PPy. In FTIR-ATR, a shoulder evolving in the  $1030\text{ cm}^{-1}$  peak was attributed to C–O, that is, C–OH vibrations. The FTIR-ATR peaks generally shifted toward higher wavenumbers due to the degradation. Specifically, the shift in the position of the peak around  $1300\text{ cm}^{-1}$  was found to correlate with the specific charge capacity of the composites. This may be a useful and quick analytical tool to measure the extent of PPy degradation, in relative terms.

In addition to the pH-dependence, electroactivity and FTIR-ATR data also showed that the degradation is less extensive, as compared to pure water, when chloride ions are added to the rinsing solution. It was also shown that the effects of nonacidic rinsing were primarily irreversible, but to a minor extent also reversible in terms of electroactivity.

The conductivity and electroactivity of extensively rinsed samples, for example, 17 L water rinsing, were constantly low during approximately 200 days of storage in ambient air, and FTIR-ATR data showed that the oxidation state was not significantly reduced during this time. Still, a carbonyl peak at  $\sim 1700\text{ cm}^{-1}$  clearly evolved over time, which thus had very little, if any, influence on the conductivity or electroactivity properties of the PPy/cellulose material. For samples rinsed with HCl, that is, those that were not degraded during rinsing, no significant amount of carbonyl groups could be detected even after  $\sim 200$  days of storage. Still, some electroactivity loss was observed in these samples as well as a minor reduction in oxidation state. Although it could not be clearly evidenced that this was due to hydroxyl group incorporation in the PPy backbone, the observed changes in the  $1030\text{ cm}^{-1}$  FTIR-ATR peak may be indicative of hydroxyl groups. The conductivity data, however, showed that samples that had not been significantly degraded during rinsing approached a limit value. For some samples, this corresponded to an  $\sim 80\%$  loss. With only minor reduction of the oxidation state of PPy, this indicates that the aqueous phase within the samples must change during the aging in ambient air. Therefore, conductivity loss is a poor indicator of PPy degradation unless the water content is controlled before measurement.

## ■ ASSOCIATED CONTENT

### § Supporting Information

Cyclic voltammograms of PPy/cellulose composites following rinsing with different solutions and volumes, with details about specific charge capacity calculations. FTIR-ATR spectra and peak positions for composite samples following rinsing. FTIR-ATR spectra for composite samples CV-cycled in 2 M NaCl at pH 12 and samples CV-cycled to overoxidation potentials in 2 M NaCl. FTIR-ATR spectra of samples following aging in ambient air. This material is available free of charge via the Internet at <http://pubs.acs.org>.

## AUTHOR INFORMATION

### Corresponding Author

\*E-mail: leif.nyholm@kemi.uu.se (L.N.); maria.stromme@angstrom.uu.se (M.S.).

### Notes

The authors declare no competing financial interest.

## ACKNOWLEDGMENTS

We thank the Swedish Foundation for Strategic Research (SSF), the Swedish Science Council (VR), the Swedish Energy Agency (Energimyndigheten), the Bo Rydin Foundation, the Nordic Innovation Centre (contract number 10014), the European Institute of Innovation and Technology under the KIC InnoEnergy NewMat, and electrical energy storage project for their financial support of this work. Dr. Johan Forsgren is kindly acknowledged for help with collecting XPS data and Prof. Håkan Rensmo for valuable discussions.

## REFERENCES

- (1) Inzelt, G. *Conducting Polymers: A New Era in Electrochemistry*; Springer: Berlin, 2008.
- (2) Sasso, C.; Beneventi, D.; Zeno, E.; Chaussy, D.; Petit-Conil, M.; Belgacem, N. Polypyrrole and Polypyrrole/Wood-Derived Materials Conducting Composites: A Review. *BioResources* **2011**, *6*, 3585–3620.
- (3) Wallace, G. G.; Spinks, G. M.; Kane-Maguire, L. A. P.; Teasdale, P. R. *Conductive Electroactive Polymers: Intelligent Polymer Systems*, 3rd ed.; CRC Press: Boca Raton, FL, 2008.
- (4) Ansari, R. Polypyrrole Conducting Electroactive Polymers: Synthesis and Stability Studies. *E-J. Chem.* **2006**, *3*, 186–201.
- (5) Ko, J. M.; Rhee, H. W.; Park, S. M.; Kim, C. Y. Morphology and Electrochemical Properties of Polypyrrole Films Prepared in Aqueous and Nonaqueous Solvents. *J. Electrochem. Soc.* **1990**, *137*, 905–909.
- (6) Razaq, A.; Mihranyan, A.; Welch, K.; Nyholm, L.; Strømme, M. Influence of the Type of Oxidant on Anion Exchange Properties of Fibrous Cladophora Cellulose/Polypyrrole Composites. *J. Phys. Chem. B* **2009**, *113*, 426–433.
- (7) Sadki, S.; Schottland, P.; Brodie, N.; Sabouraud, G. The Mechanisms of Pyrrole Electropolymerization. *Chem. Soc. Rev.* **2000**, *29*, 283–293.
- (8) Wang, L. X.; Li, X. G.; Yang, Y. L. Preparation, Properties and Applications of Polypyrroles. *React. Funct. Polym.* **2001**, *47*, 125–139.
- (9) Nyström, G.; Razaq, A.; Strømme, M.; Nyholm, L.; Mihranyan, A. Ultrafast All-Polymer Paper-Based Batteries. *Nano Lett.* **2009**, *9*, 3635–3639.
- (10) Mihranyan, A.; Nyholm, L.; Garcia-Bennett, A. E.; Strømme, M. Novel High Specific Surface Area Conducting Paper Material Composed of Polypyrrole and Cladophora Cellulose. *J. Phys. Chem. B* **2008**, *112*, 12249–12255.
- (11) Nyström, G.; Strømme, M.; Sjödin, M.; Nyholm, L. Rapid Potential Step Charging of Paper-Based Polypyrrole Energy Storage Devices. *Electrochim. Acta* **2012**, *70*, 91–97.
- (12) Olsson, H.; Nyström, G.; Strømme, M.; Sjödin, M.; Nyholm, L. Cycling Stability and Self-Protective Properties of a Paper-Based Polypyrrole Energy Storage Device. *Electrochem. Commun.* **2011**, *13*, 869–871.
- (13) Razaq, A.; Nyholm, L.; Sjödin, M.; Strømme, M.; Mihranyan, A. Paper-Based Energy Storage Devices Comprising Carbon Fibre-Reinforced Polypyrrole-Cladophora Nanocellulose Composite Electrodes. *Adv. Energy Mater.* **2012**, *2*, 445–454.
- (14) Gelin, K.; Mihranyan, A.; Razaq, A.; Nyholm, L.; Strømme, M. Potential Controlled Anion Absorption in a Novel High Surface Area Composite of Cladophora Cellulose and Polypyrrole. *Electrochim. Acta* **2009**, *54*, 3394–3401.
- (15) Strømme, M.; Frenning, G.; Razaq, A.; Gelin, K.; Nyholm, L.; Mihranyan, A. Ionic Motion in Polypyrrole-Cellulose Composites: Trap Release Mechanism During Potentiostatic Reduction. *J. Phys. Chem. B* **2009**, *113*, 4582–4589.
- (16) Razaq, A.; Strømme, M.; Nyholm, L.; Mihranyan, A. Electrochemically Controlled Separation of DNA Oligomers with High Surface Area Conducting Paper Electrode. *ECS Trans.* **2011**, *35*, 135–142.
- (17) Rubino, S.; Razaq, A.; Nyholm, L.; Strømme, M.; Leifer, K.; Mihranyan, A. Spatial Mapping of Elemental Distributions in Polypyrrole-Cellulose Nanofibers Using Energy-Filtered Transmission Electron Microscopy. *J. Phys. Chem. B* **2010**, *114*, 13644–13649.
- (18) Razaq, A.; Nyström, G.; Strømme, M.; Mihranyan, A.; Nyholm, L. High-Capacity Conductive Nanocellulose Paper Sheets for Electrochemically Controlled Extraction of DNA Oligomers. *PLoS One* **2011**, *6*, e29243.
- (19) Ferraz, N.; Carlsson, D. O.; Hong, J.; Larsson, R.; Fellström, B.; Nyholm, L.; Strømme, M.; Mihranyan, A. Haemocompatibility and Ion Exchange Capability of Nanocellulose Polypyrrole Membranes Intended for Blood Purification. *J. R. Soc., Interface* **2012**, *9*, 1943–1955.
- (20) Ferraz, N.; Strømme, M.; Fellström, B.; Nyholm, L.; Mihranyan, A. In Vitro and in Vivo Toxicity of Rinsed and Aged Nanocellulose-Polypyrrole Composites. *J. Biomed. Mater. Res., Part A* **2012**, *100 A*, 2128–2138.
- (21) Carlsson, D. O.; Nyström, G.; Zhou, Q.; Berglund, L. A.; Nyholm, L.; Strømme, M. Electroactive Nanofibrillated Cellulose Aerogel Composites with Tunable Structural and Electrochemical Properties. *J. Mater. Chem.* **2012**, *22*, 19014–19024.
- (22) Niu, J.; Conway, B. E.; Pell, W. G. Comparative Studies of Self-Discharge by Potential Decay and Float-Current Measurements at C Double-Layer Capacitor and Battery Electrodes. *J. Power Sources* **2004**, *135*, 332–343.
- (23) Novak, P.; Inganäs, O. Self-Discharge Rate of the Polypyrrole-Polyethylene Oxide Composite Electrode. *J. Electrochem. Soc.* **1988**, *135*, 2485–2490.
- (24) Chehimi, M. M.; Abdeljalil, E. A Study of the Degradation and Stability of Polypyrrole by Inverse Gas Chromatography, X-Ray Photoelectron Spectroscopy, and Conductivity Measurements. *Synth. Met.* **2004**, *145*, 15–22.
- (25) Mansouri, J.; Burford, R. P. Characterization of PVDF-PPY Composite Membranes. *Polymer* **1997**, *38*, 6055–6069.
- (26) Novák, P. Limitations of Polypyrrole Synthesis in Water and Their Causes. *Electrochim. Acta* **1992**, *37*, 1227–1230.
- (27) Thieblemont, J. C.; Planche, M. F.; Petrescu, C.; Bouvier, J. M.; Bidan, G. Stability of Chemically Synthesized Polypyrrole Films. *Synth. Met.* **1993**, *59*, 81–96.
- (28) Machida, S.; Miyata, S.; Techagumpuch, A. Chemical Synthesis of Highly Electrically Conductive Polypyrrole. *Synth. Met.* **1989**, *31*, 311–318.
- (29) Alumaa, A.; Hallik, A.; Sammelselg, V.; Tamm, J. On the Improvement of Stability of Polypyrrole Films in Aqueous Solutions. *Synth. Met.* **2007**, *157*, 485–491.
- (30) Beck, F.; Barsch, U.; Michaelis, R. Corrosion of Conducting Polymers in Aqueous-Media. *J. Electroanal. Chem.* **1993**, *351*, 169–184.
- (31) Beck, F.; Michaelis, R. Corrosion of Synthetic Metals. *Mater. Corros.* **1991**, *42*, 341–347.
- (32) Ge, H.; Qi, G.; Kang, E.-T.; Neoh, K. G. Study of Overoxidized Polypyrrole Using X-Ray Photoelectron Spectroscopy. *Polymer* **1994**, *35*, 504–508.
- (33) Ghosh, S.; Bowmaker, G. A.; Cooney, R. P.; Seakins, J. M. Infrared and Raman Spectroscopic Studies of the Electrochemical Oxidative Degradation of Polypyrrole. *Synth. Met.* **1998**, *95*, 63–67.
- (34) Li, Y.; Qian, R. Electrochemical Overoxidation of Conducting Polypyrrole Nitrate Film in Aqueous Solutions. *Electrochim. Acta* **2000**, *45*, 1727–1731.
- (35) Malitesta, C.; Losito, I.; Sabbatini, L.; Zamboni, P. G. New Findings on Polypyrrole Chemical Structure by XPS Coupled to Chemical Derivatization Labelling. *J. Electron Spectrosc. Relat. Phenom.* **1995**, *76*, 629–634.

- (36) Neoh, K. G.; Young, T. T.; Kang, E. T.; Kang, T. Structural and Mechanical Degradation of Polypyrrole Films Due to Aqueous Media and Heat Treatment and the Subsequent Redoping Characteristics. *J. Appl. Polym. Sci.* **1997**, *64*, 519–526.
- (37) Novak, P.; Rasch, B.; Vielstich, W. Overoxidation of Polypyrrole in Propylene Carbonate - an In Situ FTIR Study. *J. Electrochem. Soc.* **1991**, *138*, 3300–3304.
- (38) Palmisano, F.; Malitesta, C.; Centonze, D.; Zamboni, P. G. Correlation between Permselectivity and Chemical Structure of Overoxidized Polypyrrole Membranes Used in Electroproduced Enzyme Biosensors. *Anal. Chem.* **1995**, *67*, 2207–2211.
- (39) Rodríguez, I.; Scharifker, B. R.; Mostany, J. In Situ FTIR Study of Redox and Overoxidation Processes in Polypyrrole Films. *J. Electroanal. Chem.* **2000**, *491*, 117–125.
- (40) Schlenoff, J. B.; Xu, H. Evolution of Physical and Electrochemical Properties of Polypyrrole During Extended Oxidation. *J. Electrochem. Soc.* **1992**, *139*, 2397–2401.
- (41) Xie, H.; Yan, M.; Jiang, Z. Transition of Polypyrrole from Electroactive to Electroinactive State Investigated by Use of in Situ FTIR Spectroscopy. *Electrochim. Acta* **1997**, *42*, 2361–2367.
- (42) Park, D. S.; Shim, Y. B.; Park, S. M. Degradation of Electrochemically Prepared Polypyrrole in Aqueous Sulfuric Acid. *J. Electrochem. Soc.* **1993**, *140*, 609–614.
- (43) Erlandsson, R.; Inganäs, O.; Lundström, I.; Salaneck, W. R. XPS and Electrical Characterization of  $\text{BF}_4$ -Doped Polypyrrole Exposed to Oxygen and Water. *Synth. Met.* **1985**, *10*, 303–318.
- (44) Kudoh, Y.; Fukuyama, M.; Yoshimura, S. Stability Study of Polypyrrole and Application to Highly Thermostable Aluminum Solid Electrolytic Capacitor. *Synth. Met.* **1994**, *66*, 157–164.
- (45) Münsterdt, H. Ageing of Electrically Conducting Organic Materials. *Polymer* **1988**, *29*, 296–302.
- (46) Brie, M.; Turcu, R.; Mihut, A. Stability Study of Conducting Polypyrrole Films and Polyvinylchloride-Polypyrrole Composites Doped with Different Counterions. *Mater. Chem. Phys.* **1997**, *49*, 174–178.
- (47) Benseddik, E.; Makhoul, M.; Bernede, J. C.; Lefrant, S.; Pron, A. XPS Studies of Environmental Stability of Polypyrrole-Poly(Vinyl Alcohol) Composites. *Synth. Met.* **1995**, *72*, 237–242.
- (48) Mhryanyan, A.; Llagostera, A. P.; Karmhag, R.; Strømme, M.; Ek, R. Moisture Sorption by Cellulose Powders of Varying Crystallinity. *Int. J. Pharm.* **2004**, *269*, 433–442.
- (49) Beamson, G.; Briggs, D. *High Resolution XPS of Organic Polymers: The Scienta ESCA 300 Database*; John Wiley & Sons Ltd.: Chichester, 1992.
- (50) Maia, G.; Ticianelli, E. A.; Nart, F. C. FTIR Investigation of the Polypyrrole Oxidation in  $\text{Na}_2\text{SO}_4$  and  $\text{NaNO}_3$  Aqueous-Solutions. *Z. Phys. Chem.* **1994**, *186*, 245–257.
- (51) Olsson, H.; Carlsson, D. O.; Nyström, G.; Sjödin, M.; Nyholm, L.; Strømme, M. Influence of the Cellulose Substrate on the Electrochemical Properties of Paper-Based Polypyrrole Electrode Materials. *J. Mater. Sci.* **2012**, *47*, 5317–5325.
- (52) Goormaghtigh, E.; Raussens, V.; Ruysschaert, J. M. Attenuated Total Reflection Infrared Spectroscopy of Proteins and Lipids in Biological Membranes. *Biochim. Biophys. Acta, Rev. Biomembr.* **1999**, *1422*, 105–185.
- (53) Lee, C.; Kwak, J.; Bard, A. J. Polymer Films on Electrodes. Xxiv. Ellipsometric Study of the Electrochemical Redox Process of a Polypyrrole Film on a Platinum Electrode. *J. Electrochem. Soc.* **1989**, *136*, 3720–3723.